



Superconductivity in a single-layer alkali-doped FeSe: A weakly coupled two-leg ladder system

Wei Li,^{1,*} Hao Ding,¹ Pengfei Zhang,¹ Peng Deng,¹ Kai Chang,¹ Ke He,² Shuaihua Ji,¹ Lili Wang,² Xucun Ma,² Jian Wu,¹ Jiang-Ping Hu,² Qi-Kun Xue,^{1,†} and Xi Chen^{1,‡}

¹State Key Laboratory of Low-Dimensional Quantum Physics, Department of Physics, Tsinghua University, Beijing 100084, China

²Institute of Physics, Chinese Academy of Sciences, Beijing 100190, China

(Received 14 October 2012; revised manuscript received 6 October 2013; published 21 October 2013)

We prepare single-layer potassium-doped iron selenide (110) film by molecular-beam epitaxy. Such a single-layer film can be viewed as a two-dimensional system composed of weakly coupled two-leg iron ladders. Scanning tunneling spectroscopy reveals that superconductivity is developed in this two-leg ladder system. The superconducting gap is similar to that of the multilayer films. However, the Fermi-surface topology in this quasi-one-dimensional system is remarkably different from that of the bulk materials. Our results suggest that superconducting pairing is very short ranged or takes place rather locally in iron chalcogenides. The superconductivity is most likely driven by electron-electron correlation effect and is insensitive to the change of Fermi surfaces.

DOI: 10.1103/PhysRevB.88.140506

PACS number(s): 74.70.Xa, 73.20.-r, 74.55.+v, 74.78.-w

In spite of intensive investigation, there is still no consensus on whether a strong-coupling or a weak-coupling model is more appropriate for describing high-temperature superconductivity. For the recently discovered iron-based superconductors,^{1–4} such an issue is still an open debate as well.^{5–19} In the strong-coupling picture, the essential physics of high- T_c superconductivity is expected to be understood in terms of localized models. Alternatively, a weak-coupling model begins by considering the energy bands and Fermi surface. One approach to addressing this problem is to discover and study high T_c superconductors with reduced dimensionality. For example, quasi-one-dimensional systems, such as ladder or chain materials, are simple model systems for theories of superconductivity based on magnetic pairing mechanisms.^{20–23} Experimentally, the only spin-ladder system found to be superconducting so far is $\text{Sr}_{14-x}\text{Ca}_x\text{Cu}_{24}\text{O}_{41}$ ($x = 11.5\text{--}15.5$).^{24,25} However, the origin of superconductivity in this ladder material is still controversial because it becomes superconducting only by applying high pressure, which may change one-dimensional physics. Here we report on the superconductivity in a single layer $\text{K}_x\text{Fe}_{2-y}\text{Se}_2$ (110) film. The single layer $\text{K}_x\text{Fe}_{2-y}\text{Se}_2$ (110) is a two-dimensional system composed of weakly coupled two-leg iron ladders. The finding indicates that superconducting pairing is very short ranged and most likely driven by electron-electron correlation effect in iron chalcogenides.

The single-layer $\text{K}_x\text{Fe}_{2-y}\text{Se}_2$ along the [110] direction was grown by molecular-beam epitaxy (MBE). The (001) plane is the natural cleavage plane of the layered material $\text{K}_x\text{Fe}_{2-y}\text{Se}_2$ and the (110) plane shows the cross section. The (001) oriented single-layer film can be viewed as a two-dimensional system composed of weakly coupled two-leg iron ladders [Fig. 1(a)]. Using scanning tunneling microscopy (STM) and spectroscopy (STS), we demonstrate that a superconducting gap is developed and the gap size is reduced by only 10% compared with that of a multilayer film.²⁶ The prominent advantage of the single-layer $\text{K}_x\text{Fe}_{2-y}\text{Se}_2$ over other ladder systems is that this system is obtained by reducing the dimensionality (especially the in-plane dimensionality) of an existing bulk superconductor. The two-leg Fe ladder can be

considered as the building block of both bulk and single-layer $\text{K}_x\text{Fe}_{2-y}\text{Se}_2$, and provides an opportunity to study the dimensionality effect and therefore casts new light on resolving the controversy between strong-coupling and weak-coupling models. By studying the superconductivity in this ladder system, we show that superconducting pairing in iron-based superconductors stems from local short-ranged microscopic energetics rather than the Fermi-surface properties.

The experiments were performed on a Unisoku ultrahigh vacuum STM system at base temperature of 0.4 K by means of a single-shot ³He cryostat. A magnetic field up to 11 T can be applied perpendicular to the sample surface. A polycrystalline PtIr STM tip was used in the STM measurement. The system has an MBE chamber for thin-film growth. High purity Fe (99.995%), Se (99.9999%), and K were evaporated simultaneously from two standard Knudsen cells and one alkali-metal dispenser (SAES Getters). The temperatures of Fe cell and Se cell were chosen to be 1250 and 165 °C, respectively, leading to a low growth rate of about 0.1 unit cell per minute. The K flux is relatively flexible and determines the area ratio of the KFe_2Se_2 phase and $\text{K}_2\text{Fe}_4\text{Se}_5$ phase.²⁶ In order to obtain the single-layer $\text{K}_x\text{Fe}_{2-y}\text{Se}_2$ (110) islands, the substrate was held at 440 °C for 10 min during growth. The sample was subsequently annealed at 470 °C for 3 h. The background pressure is better than 1×10^{-9} Torr during growth.

The single layer (110) films of $\text{K}_x\text{Fe}_{2-y}\text{Se}_2$ (110) [Fig. 1(b)] were obtained on graphitized 6H-SiC(0001) under well-controlled growth conditions. The substrate [dark region in Fig. 1(b)] is bilayer graphene, characterized by the 6×6 hexagonal superstructure²⁷ [Fig. 1(c)] and a typical gap-like feature in the dI/dV spectrum²⁸ (see Supplemental Material²⁹). Similar to our previous studies,^{26,30} two distinct regions known as insulating 245 phase with $\sqrt{5} \times \sqrt{5}$ Fe vacancy order [Fig. 1(d)] and conducting 122 phase [Fig. 1(e)] are clearly revealed on the island, indicating that phase separation occurs at the single-layer level as well. The two phases always coexist side by side. In a single layer, the composition of $\text{K}_x\text{Fe}_{2-y}\text{Se}_2$ (110) in the 122 phase actually becomes $\text{K}_3\text{Fe}_4\text{Se}_6$ instead of KFe_2Se_2 . Therefore we will use “346” to label the conducting phase of single-layer $\text{K}_x\text{Fe}_{2-y}\text{Se}_2$.

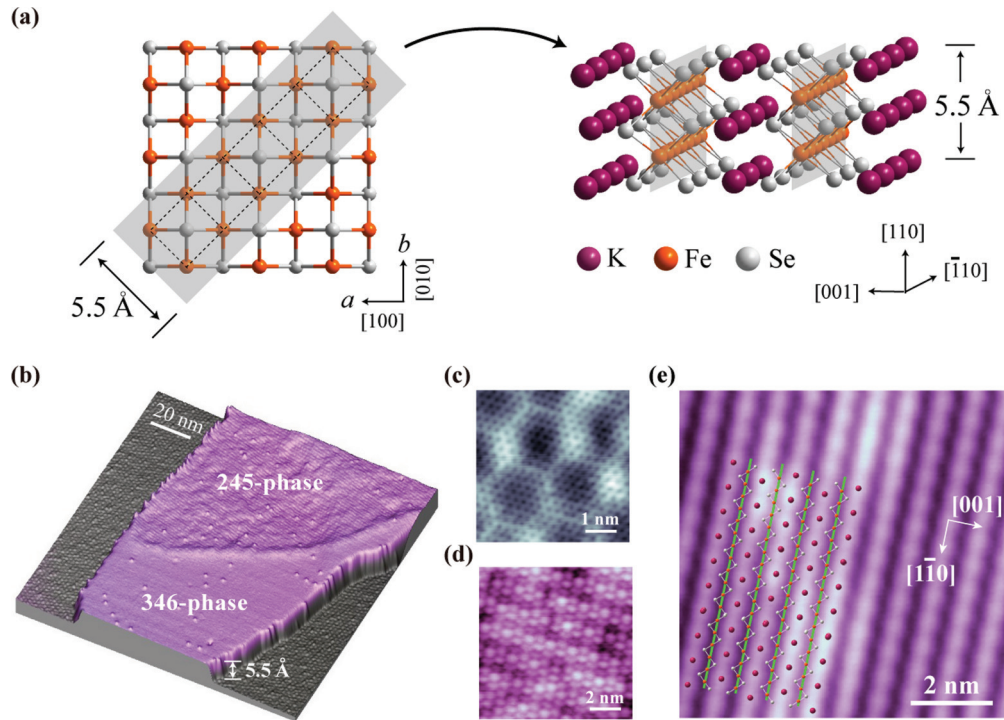


FIG. 1. (Color online) Single-layer $K_xFe_{2-y}Se_2(110)$. (a) Two-leg ladder system composed of weakly coupled iron atom chains. The same convention for Miller indices is used throughout. In the single layer two-leg ladder system (schematic on right), each FeSe(001) layer contributes one ladder (the shaded area in the schematic on left, dashed lines marked the Fe ladder), which is along the $[\bar{1}10]$ direction. A layer of K atoms is sandwiched between two ladders. (b) STM topographic image ($150\text{ nm} \times 150\text{ nm}$, 3.9 V , 0.02 nA) of a single layer $K_xFe_{2-y}Se_2(110)$ island. Two distinct regions are marked by 346 phase and 245 phase. The apparent height of island is insensitive to bias voltage from 0.5 to 4.0 V and estimated to be $5.5 \pm 0.3\text{ \AA}$. The substrate is bilayer graphene characterized by 6×6 hexagonal superstructure (c). (d) STM image of 245 phase (1.35 V , 0.03 nA). The periodic stripe pattern is attributed to the $\sqrt{5} \times \sqrt{5}$ Fe vacancy order seen along the $[110]$ direction. (e) STM image of 122 phase ($8\text{ nm} \times 8\text{ nm}$, 10 mV , 0.02 nA). The locations of iron ladders are marked by dashed lines. The locations of K and Se atoms are marked by red and white dots, respectively.

We focus on the 346 phase, which is superconducting in the case of multilayer films. Along the $[110]$ direction, a single-layer $K_3Fe_4Se_6(110)$ contains one complete unit cell of the 122 phase and its thickness is 5.5 \AA [see Figs. 1(a) and 1(b)]. The (110) plane is terminated with K and Se atoms. The K atoms form atomic rows and are visible at positive bias in the STM image [Fig. 1(e)]. Each of the weakly coupled two-leg iron ladders is located in the middle between two adjacent K atom rows. This unique configuration provides an ideal platform to explore superconductivity in ladder systems.

STS probes the local density of states of quasiparticles. In Fig. 2(a), the STS measurements on single-layer 346 phase at 0.4 K show clear evidence of superconductivity in this two-leg ladder system. The gap is centered at the Fermi level and has two coherence peaks. Similar to the spectrum acquired on a multilayer sample [dashed curve in Fig. 2(a) and also Ref. 26], the STS reveals a double-gap structure as well. Despite the reduced dimensionality, the spectrum does not greatly change, indicating that the gap observed in the 346 phase has the same origin as that in the bulk superconducting 122 phase. The coherence peaks for the single-layer 346 phase are slightly broadened and the superconducting gap is reduced from 4.0 meV for the multilayer film to 3.6 meV . The spectra always exhibit a finite zero-bias conductance most likely because of

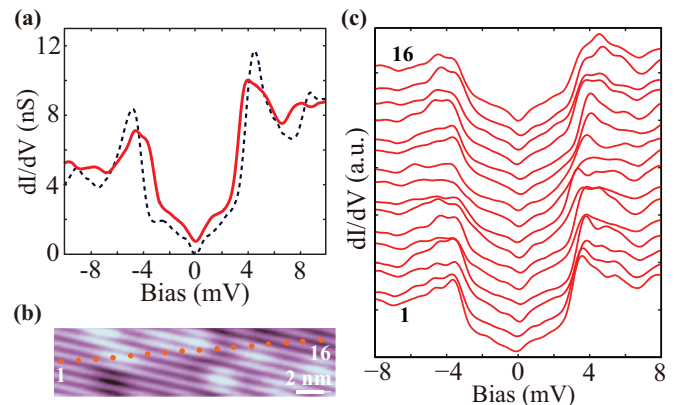


FIG. 2. (Color online) Superconductivity in single layer 346 phase. (a) The superconducting gap (solid curve) of single layer 346 phase. Set point: 14 mV and 0.1 nA . Temperature: 0.4 K . The modulation amplitude and frequency for lock-in measurement are 0.3 mV and 931 Hz . For comparison, the spectrum for multilayer 122 phase (dashed curve) is shown. (b) A $5\text{ nm} \times 25\text{ nm}$ topography image (14 mV , 0.1 nA) of the superconducting region. The area shown here is part of the region in Fig. 1(b). Inhomogeneity in electronic structure is revealed. (c) A series of dI/dV spectra measured at 16 points indicated in (b). Set point: 14 mV and 0.1 nA . The spectra are offset for clarity.

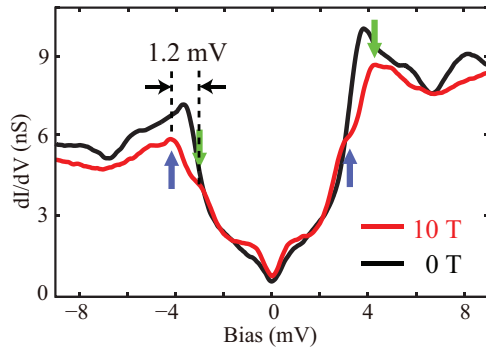


FIG. 3. (Color online) Magnetic field splitting of the quasiparticle states. dI/dV spectra show density of states for single-layer 346 phase at 0 and 10 T, respectively. Set point: 14 mV, 0.1 nA. The coherence peaks are split into spin-up and spin-down components under magnetic field.

the quasiparticle scattering from the substrate. The thickness of the film is only 5.5 Å and much shorter than the coherence length of the 346 phase in the a - b plane. Thus the influence of the substrate is not negligible.

While structural defects are rarely found in the single-layer film, inhomogeneity in electronic structure commonly exists as shown in the STM image [Fig. 2(b)]. A series of dI/dV spectra taken along the dotted line in Fig. 2(b) also exhibit small variation of superconducting gap at different locations. Such inhomogeneity does not present in multilayer films²⁶ and can be attributed to the inhomogeneity of electronic structure of the graphitized SiC substrate.

Besides the substrate, the superconducting gap is susceptible to external magnetic field as well (Fig. 3). When a magnetic field is applied parallel to a very thin film or to a type-II superconductor, the effect of field on spins dominates the one on orbits.³¹ At the Pauli limit, where Zeeman energy is comparable to the superconducting gap, the Cooper pairs are broken. Below the Pauli limit, the spectrum simply shifts by a Zeeman term in energy. One coherence peak splits into the up and down spin states and the splitting is given by $2\mu_B B$, where μ_B is the Bohr magneton. This effect has been observed experimentally in thin superconducting aluminum films.^{32–36} In the single-layer 346 phase, the splitting at 10 T is 1.2 meV (Fig. 3), close to the theoretical value 1.16 meV. The same behavior is obtained at different locations and on multilayer film (see Supplemental Material²⁹).

Conceivably, the Fermi-surface topology of the quasi-one-dimensional ladder system should be significantly different from that of the bulk $K_x\text{Fe}_{2-y}\text{Se}_2$, which implies that the electronic structure in momentum space is not crucial to the formation of Cooper pairs in $K_x\text{Fe}_{2-y}\text{Se}_2$. The first-principles calculation (Fig. 4) was performed within the density functional theory using the projected augmented wave method³⁷ as implemented in the VASP code.³⁸ The Perdew-Burke-Ernzerhof exchange correlation potential³⁹ was used. The calculation confirms that the single-layer 346 phase is a quasi-one-dimensional metal with two bands [Fig. 4(a)] crossing the Fermi surface. The ground state is antiferromagnetic (see Supplemental Material²⁹) with a large magnetic moment of $3.284\mu_B$ per Fe atom. The Fermi surface [Fig. 4(a)] is very

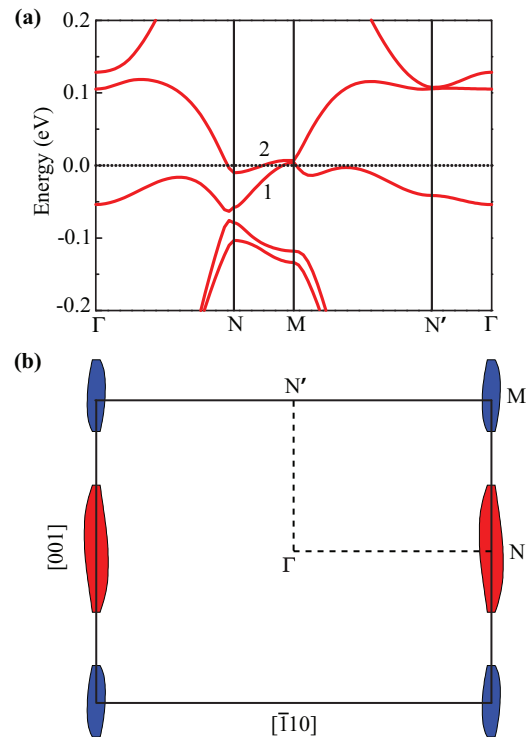


FIG. 4. (Color online) First-principles calculation of single-layer $\text{K}_3\text{Fe}_4\text{Se}_6$. A 500-eV cutoff in the plane-wave expansion ensures the calculations converge to 10^{-5} eV. For each magnetic configuration, all atomic positions and the lattice constants were optimized until the largest force on each atom is 0.01 eV/Å. A $12 \times 12 \times 1$ Monkhorst-Pack k -grid Brillouin zone is sampled throughout all calculations while the Gaussian smearing technique is used in the case of metallic states. To model the thin film, a supercell of slab is used with periodic boundary conditions in all three dimensions with a 10-Å-thick vacuum layer between two slabs in order to eliminate the interslab interactions. (a) The band structure. There are two bands crossing the Fermi surface. (b) Fermi-surface sheets. The electron and hole pockets are located at N and M points respectively. The Fermi energy sets to zero.

different from those of bulk iron based superconductors. On the boundary of the Brillouin zone, there is one electron pocket at the N point and one hole pocket at the M points. They are highly elongated along the direction perpendicular to the ladders.

Our results on single-layer two-leg ladder system have important implications. First of all, the development of superconductivity in such a low dimensional system indicates that superconducting pairing is very short ranged or takes place rather locally in iron chalcogenides. The superconductivity is most likely driven by electron-electron correlation effect and is insensitive to the Fermi-surface topology. The results strongly support earlier theoretical calculations performed on an iron-pnictide superconductor in a two-leg ladder model,^{18,40} which suggests that the underlying pairing mechanism for iron-pnictide superconductors is similar to that for the cuprates. Although those calculations were done for iron pnictides, there is a good reason to expect their validity for iron chalcogenides without significant modification. For example, recently it has been shown that the underlining kinematics between iron

pnictides and iron chalcogenides has little difference and the similarity between iron-based superconductors and cuprates can be extended to a fully two-dimensional model.¹⁹ A two-leg ladder system is exactly the minimum one-dimensional model to capture the essential physics of iron-based superconductors.

In summary, we observe superconductivity in a single-layer alkali-doped iron selenide, which is a nature-made weakly

coupled two-leg ladder system. Our results indicate that the material is a strongly correlated electron system with very short-ranged local superconducting pairing.

The work was supported by NSFC and the National Basic Research Program of China. The STM topographic images were processed using WSxM (www.nanotec.es).

*Present address: Department of Physics, Stanford University, Stanford, CA 94305.

[†]qkxue@mail.tsinghua.edu.cn

[‡]xc@mail.tsinghua.edu.cn

¹Y. Kamihara, T. Watanabe, M. Hirano, and H. Hosono, *J. Am. Chem. Soc.* **130**, 3296 (2008).

²X. H. Chen, T. Wu, G. Wu, R. H. Liu, H. Chen, and D. F. Fang, *Nature (London)* **453**, 761 (2008).

³G. F. Chen, Z. Li, D. Wu, G. Li, W. Z. Hu, J. Dong, P. Zheng, J. L. Luo, and N. L. Wang, *Phys. Rev. Lett.* **100**, 247002 (2008).

⁴J. G. Guo, S. F. Jin, G. Wang, S. C. Wang, K. X. Zhu, T. T. Zhou, M. He, and X. L. Chen, *Phys. Rev. B* **82**, 180520 (2010).

⁵J. Dong, H. J. Zhang, G. Xu, Z. Li, G. Li, W. Z. Hu, D. Wu, G. F. Chen, X. Dai, J. L. Luo, Z. Fang, and N. L. Wang, *Europhys. Lett.* **83**, 27006 (2008).

⁶I. I. Mazin, D. J. Singh, M. D. Johannes, and M. H. Du, *Phys. Rev. Lett.* **101**, 057003 (2008).

⁷K. Kuroki, S. Onari, R. Arita, H. Usui, Y. Tanaka, H. Kontani, and H. Aoki, *Phys. Rev. Lett.* **101**, 087004 (2008).

⁸F. Wang, H. Zhai, Y. Ran, A. Vishwanath, and D. H. Lee, *Phys. Rev. Lett.* **102**, 047005 (2009).

⁹R. Thomale, C. Platt, J. P. Hu, C. Honerkamp, and B. A. Bernevig, *Phys. Rev. B* **80**, 180505 (2009).

¹⁰R. Thomale, C. Platt, W. Hanke, J. P. Hu, and B. A. Bernevig, *Phys. Rev. Lett.* **107**, 117001 (2011).

¹¹A. V. Chubukov, D. V. Efremov, and I. Eremin, *Phys. Rev. B* **78**, 134512 (2008).

¹²V. Cvetkovic and Z. Tesanovic, *Phys. Rev. B* **80**, 024512 (2009).

¹³K. J. Seo, B. A. Bernevig, and J. P. Hu, *Phys. Rev. Lett.* **101**, 206404 (2008).

¹⁴Q. Si and E. Abrahams, *Phys. Rev. Lett.* **101**, 076401 (2008).

¹⁵C. Fang, H. Yao, W. F. Tsai, J. P. Hu, and S. A. Kivelson, *Phys. Rev. B* **77**, 224509 (2008).

¹⁶F. Ma, Z.-Y. Lu, and T. Xiang, *Phys. Rev. B* **78**, 224517 (2008).

¹⁷J. P. Hu and H. Ding, *Sci. Rep.* **2**, 381 (2012).

¹⁸E. Berg, S. A. Kivelson, and D. J. Scalapino, *Phys. Rev. B* **81**, 172504 (2010).

¹⁹J. P. Hu and N. Hao, *Phys. Rev. X* **2**, 021009 (2012).

²⁰E. Dagotto and T. M. Rice, *Science* **271**, 618 (1996).

²¹S. Gopalan, T. M. Rice, and M. Sigrist, *Phys. Rev. B* **49**, 8901 (1994).

²²M. Troyer, H. Tsunetsugu, and T. M. Rice, *Phys. Rev. B* **53**, 251 (1996).

²³D. J. Scalapino, *Physica B* **318**, 92 (2002).

²⁴M. Uehara, T. Nagata, J. Akimitsu, H. Takahashi, N. Mori, and K. Kinoshita, *J. Phys. Soc. Jpn.* **65**, 2764 (1996).

²⁵M. Arai and H. Tsunetsugu, *Phys. Rev. B* **56**, R4305 (1997).

²⁶W. Li, H. Ding, P. Deng, K. Chang, C. Song, K. He, L. Wang, X. Ma, J.-P. Hu, X. Chen, and Q.-K. Xue, *Nat. Phys.* **8**, 126 (2012).

²⁷P. Mallet, F. Varchon, C. Naud, L. Magaud, C. Berger, and J.-Y. Veuillen, *Phys. Rev. B* **76**, 041403(R) (2007).

²⁸Y. B. Zhang, V. W. Brar, F. Wang, C. Girit, Y. Yayon, M. Panlasigui, A. Zettl, and M. F. Crommie, *Nat. Phys.* **4**, 627 (2008).

²⁹See Supplemental Material at <http://link.aps.org/supplemental/10.1103/PhysRevB.88.140506> for additional materials about the experimental results.

³⁰W. Li, H. Ding, Z. Li, P. Deng, K. Chang, K. He, S. Ji, L. Wang, X. Ma, J.-P. Hu, Xi Chen, and Q.-K. Xue, *Phys. Rev. Lett.* **109**, 057003 (2012).

³¹P. Fulde, in *BCS: 50 Years*, edited by L. N. Cooper and D. Feldman (World Scientific, Singapore, 2011), pp. 227–253.

³²R. Meservey, P. M. Tedrow, and P. Fulde, *Phys. Rev. Lett.* **25**, 1270 (1970).

³³P. M. Tedrow and R. Meservey, *Phys. Rev. Lett.* **26**, 192 (1971).

³⁴P. M. Tedrow, J. E. Tkaczyk, and A. Kumar, *Phys. Rev. Lett.* **56**, 1746 (1986).

³⁵X. Hao, J. S. Moodera, and R. Meservey, *Phys. Rev. Lett.* **67**, 1342 (1991).

³⁶W. H. Wu, J. Williams, and P. W. Adams, *Phys. Rev. Lett.* **77**, 1139 (1996).

³⁷P. E. Blöchl, *Phys. Rev. B* **50**, 17953 (1994).

³⁸G. Kresse and J. Furthmüller, *Phys. Rev. B* **54**, 11169 (1996).

³⁹J. P. Perdew, K. Burke, and M. Ernzerhof, *Phys. Rev. Lett.* **77**, 3865 (1996).

⁴⁰E. Berg, S. A. Kivelson, and D. J. Scalapino, *New J. Phys.* **11**, 085007 (2009).